

---

# TrAME: Trajectory-Anchored Multi-View Editing for Text-Guided 3D Gaussian Splatting Manipulation

---

Chaofan Luo<sup>1,2</sup>, Donglin Di<sup>\*1</sup>, Yongjia Ma<sup>1</sup>, Zhou Xue<sup>1</sup>,  
Chen Wei<sup>1</sup>, Xun Yang<sup>\*2</sup>, Yebin Liu<sup>3</sup>

<sup>1</sup>Space AI, Li Auto; <sup>2</sup>University of Science and Technology of China; <sup>3</sup>Tsinghua University  
luocfprime@gmail.com; didonglin@lixiang.com; maguire9993@gmail.com;  
xuezhou08@gmail.com; chenwei10@lixiang.com; xyang21@ustc.edu.cn;  
liyebin@mail.tsinghua.edu.cn;

## Abstract

Despite significant strides in the field of 3D scene editing, current methods encounter substantial challenge, particularly in preserving 3D consistency in multi-view editing process. To tackle this challenge, we propose a progressive 3D editing strategy that ensures multi-view consistency via a Trajectory-Anchored Scheme (TAS) with a dual-branch editing mechanism. Specifically, TAS facilitates a tightly coupled iterative process between 2D view editing and 3D updating, preventing error accumulation yielded from text-to-image process. Additionally, we explore the relationship between optimization-based methods and reconstruction-based methods, offering a unified perspective for selecting superior design choice, supporting the rationale behind the designed TAS. We further present a tuning-free View-Consistent Attention Control (VCAC) module that leverages cross-view semantic and geometric reference from the source branch to yield aligned views from the target branch during the editing of 2D views. To validate the effectiveness of our method, we analyze 2D examples to demonstrate the improved consistency with the VCAC module. Further extensive quantitative and qualitative results in text-guided 3D scene editing indicate that our method achieves superior editing quality compared to state-of-the-art methods. We will make the complete codebase publicly available following the conclusion of the double-blind review process.

## 1 Introduction

3D technologies are pivotal in various fields, such as virtual reality (VR), the film and gaming industries, and 3D design [40, 11, 22, 12]. Recent advances in Neural Radiance Fields (NeRF) and 3D Gaussian Splatting (3DGS) have pushed the boundary of 3D representation, enabling versatile 3D applications [21, 37, 23, 31, 7, 6, 17, 35, 33, 3]. Leveraging the powerful generative capabilities of text-to-image diffusion models [2, 26], text-guided 3D editing now allows for intricate adjustments in shape, style, texture, and lighting, marking a significant advancement in the flexibility of 3D scene manipulation [9, 16, 11, 22, 12, 18].

One key challenge in 3D editing is maintaining multi-view consistency when applied to real scenes [29, 32], which is essential for preventing visual artifacts and inconsistent appearances when observed from different view angles. Current studies of 3D editing can be divided into two categories, namely optimization-based and reconstruction-based methods. The optimization-based 3D editing methods [19, 27, 20, 41, 16] usually adopt the Score Distillation Sampling (SDS) loss [25] or its modified versions [13, 24]. They often suffer from sub-optimal editing quality such as over-saturation, over-smoothing, and a lack of diversity due to the misalignment between the randomly sampled timestep  $t$

---

\*Corresponding authors.

in the SDS optimization process and the corresponding timestep  $t$  in the diffusion sampling process [15, 40]. The second category of methods, reconstruction-based 3D editing methods [9, 5, 32, 29, 18], employ readily available 2D editing diffusion models to edit 3D scene. However, 2D diffusion models struggle to achieve multi-view consistency because of their inherent limitation of independently processing each view.

In this paper, to mitigate the above-mentioned issues, we first theoretically unveil the relation between these two branches of methods, demonstrating that optimization-based methods are special cases of reconstruction-based methods. Specifically, we uncover an intrinsic equivalence between the *optimization process* of SDS [25] and an *iterative reconstruction process* that aims to match pseudo-ground-truths obtained from the Denoising Diffusion Consistent Model (DDCM) [34]. This analysis unites these two branches of 3D editing methods, offering a unified perspective for making superior design choices. Based on the analysis, we introduce a progressive 3D editing framework named “Trajectory-Anchored Multi-View Editing (TrAME)”. The core idea of this framework is the Trajectory-Anchored Scheme (TAS), a unified paradigm designed to gradually consolidate incremental 2D view edits onto 3D scenes. Inspired by an empirical practice of utilizing feedback from rendered images of the updated 3DGS to correct errors that arise during the 2D editing process [4, 42], we design TAS to enhance the interplay between the image editing process and the 3DGS update process, allowing for active rectification of inconsistencies within 2D multi-view edits through the 3D constrained rendering process (*i.e.*, rendering in the loop). Utilizing a modified DDCM editing trajectory [34], we incrementally generate pseudo-ground-truths for progressive 3D Gaussian editing. Furthermore, to enhance 3D-consistency during the 2D view editing process, we design a VCAC module with a dual-branch editing strategy. The edited views maintain *structural multi-view consistency* via self-attention queries injected from the source branch into the target branch during the early stages of diffusion. To enhance *semantic multi-view consistency*, we facilitate self-attention Key-Value (KV) propagation and KV reference mechanisms, propagating the self-attention keys and values of keyframes within the same context and inflating the self-attention keys and values across different keyframes for a mutual reference.

We conduct extensive experiments to demonstrate the effectiveness of our proposed TAS strategy and VCAC module. Both qualitative and quantitative results of 3D editing highlight the superiority of our approach in comparison to state-of-the-art methods. Additionally, the qualitative results from ablation studies demonstrate enhanced consistency with our proposed TAS and VCAC module. Our main contributions are summarized as follows:

- Our theoretical analysis bridges the gap between optimization-based and reconstruction-based editing methods, offering a unified perspective for selecting superior design choices.
- We propose a progressive 3D editing strategy that integrates a Trajectory-Anchored Scheme (TAS). This design ensures multi-view consistency by tightly coupling the iterative processes of 2D view editing and 3D scene updating, thereby preventing error accumulation during text-to-image process.
- We present a tuning-free VCAC module that enhances the 3D consistency of editing results. The VCAC leverages cross-view semantic and geometric references from the source branch to yield aligned views in the target branch via query injection, KV propagation and KV reference mechanisms.
- Extensive experimental results in text-guided 3D scene editing demonstrate that our method achieves improved multi-view consistency editing results compared with state-of-the-art methods.

## 2 Related Work

In this section, we provide a concise overview of two primary branches of methodologies employed in the task of 3D scene editing: optimization-based methods and reconstruction-based methods.

Regarding **optimization-based 3D editing**, significant advancements have been made, building upon the foundational SDS loss introduced by DreamFusion [25]. This has catalyzed the development of various innovative methods [19, 27, 20, 41, 16, 24] aimed at refining 3D model editing via optimizing the SDS loss. Notably, Vox-E [27] and DreamEditor [41] have harnessed explicit 3D representations, including voxels and meshes. These approaches utilize cross-attention mechanisms to facilitate precise manipulations within specific regions of 3D models. Furthermore, RePaint-NeRF [39] has advanced the application of SDS in 3D editing by integrating a semantic mask to guide and constrain modifications within the background elements. In a similar vein, ED-NeRF [24] has introduced an enhanced loss function specifically designed for 3D editing tasks. It extends the Delta Denoising

Score (DDS) loss [13] into the three-dimensional space, offering a more refined approach to editing. Despite these advancements, a common challenge still persists among methods that utilize randomly sampled timesteps  $t$  within the SDS framework: This approach tends to lead to deviations from the intended diffusion sampling trajectories, which can result in compromised quality of the 3D edits.

For **reconstruction-based 3D editing**, InstructN2N [9] alongside subsequent studies [5, 32, 29, 18], have leveraged advancements in 2D diffusion editing techniques, notably InstructP2P [2] and ControlNet [38], for enhancing scene updates through Iterative Dataset Update [9]. GaussianEditor [5] and GaussCtrl [32] introduce methods for precise control in partial 3D editing. GaussianEditor utilizes semantic tracing to segment the 3D Gaussians to be edited. GaussCtrl proposes depth-guided editing and attention-based latent alignment. However, these methods often neglect inter-view correlations, resulting in a gap in maintaining semantic and structural consistency across multiple views, ultimately leading to error accumulation. Our work bridges this gap by integrating Trajectory-Anchored Scheme to minimize error accumulation and introducing attention manipulation mechanisms to enforce structural and semantic consistency across views in 3D editing through our VCAC module.

### 3 Preliminaries

In this section, we first briefly review Score Distillation Sampling (SDS) and Denoising Diffusion Consistent Model (DDCM) before delving into the analysis of the relation between optimization-based editing and reconstruction-based editing.

#### 3.1 Score Distillation Sampling

Score Distillation Sampling (SDS) [25], also known as Score Jacobian Chaining (SJC) [30], is a commonly adopted technique in 3D asset generation and editing. It performs sampling in parameter space by optimizing a diffusion distillation loss function. Given a camera pose  $c$  and the parameters of a 3D representation  $\theta$ , noisy latents  $z_t$  are obtained by first rendering different views and then adding noise to the latents of the rendered images. The gradient with respect to the parameter of the 3D representation  $\theta$  is defined as in Eq. 1, using a pretrained diffusion model  $\epsilon_\phi$  to predict the noise estimate conditioned by  $y$  and match it against the ground truth noise  $\epsilon$ . This gradient is backpropagated through a differentiable render function  $g(\cdot, c)$ , scaled by a weighting schedule  $\omega(t)$ .

$$\nabla_\theta \mathcal{L}_{\text{SDS}}(\theta) := \mathbb{E}_{t, \epsilon, c} \left[ \omega(t) (\epsilon_\phi(z_t, t, y) - \epsilon) \frac{\partial g(\theta, c)}{\partial \theta} \right]. \quad (1)$$

Additionally, variant loss functions, such as Delta Denoising Score, are often used as a substitute for the vanilla SDS loss.

#### 3.2 Denoising Diffusion Consistent Model

Denoising Diffusion Implicit Models (DDIMs) [28] characterize a family of generative models with non-Markovian forward processes. Given a noisy latent  $z_t$  with condition  $y$  at timestep  $t$ , the sampling procedure of DDIM is formulated as:

$$z_{t-1} = \underbrace{\sqrt{\alpha_{t-1}} \left( \frac{z_t - \sqrt{1 - \alpha_t} \epsilon_\phi(z_t, t, y)}{\sqrt{\alpha_t}} \right)}_{\text{predicted } \hat{z}_0^{(t)}} + \underbrace{\sqrt{1 - \alpha_{t-1} - \sigma_t^2} \cdot \epsilon_\phi(z_t, t, y)}_{\text{direction pointing to } z_t} + \underbrace{\sigma_t \epsilon_t}_{\text{random noise}}, \quad (2)$$

where  $\epsilon_\phi$  is the noise predictor parameterized by parameter  $\phi$  and  $\alpha_t$  corresponds to diffusion schedule. Different instances of  $\sigma_t$  in Eq. 2 yield different generative processes [28]. Consider a special generative process where  $\sigma_t := \sqrt{1 - \alpha_{t-1}}$ . The second term on the right-hand side of Eq. 2 is canceled out, leaving only  $\hat{z}_0^{(t)}$  and the newly added noise  $\sigma_t \epsilon_t$ :

$$z_{t-1} = \sqrt{\alpha_{t-1}} \left( \frac{z_t - \sqrt{1 - \alpha_t} \epsilon_\phi(z_t, t, y)}{\sqrt{\alpha_t}} \right) + \sqrt{1 - \alpha_{t-1}} \epsilon_t, \quad (3)$$

which is formulated as Denoising Diffusion Consistent Model (DDCM) [34].

## 4 Methodology

We first analyze the relation between optimization-based and reconstruction-based 3D scene editing methods in detail. Then, we elaborate on the proposed progressive Trajectory-Anchored Scheme (TAS) and the design of View-Consistent Attention Control (VCAC). The overall framework is illustrated in Figure 1.

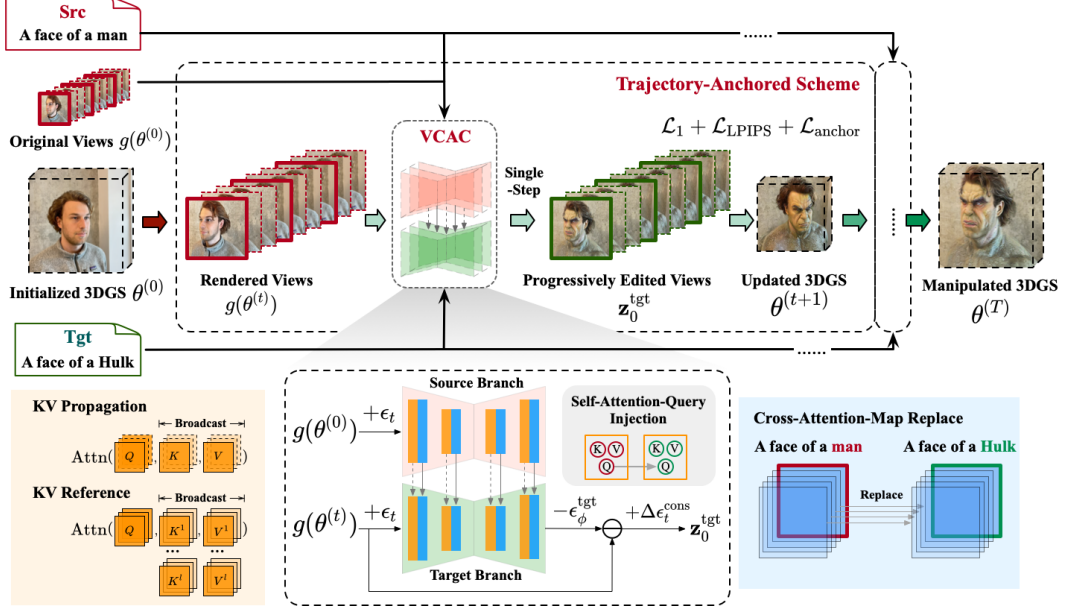


Figure 1: Illustration of the proposed method, Trajectory-Anchored Multi-View Editing for 3D Gaussian Splatting Manipulation (TrAME). Our method comprises a Trajectory Anchored Scheme (TAS) as well as a View-Consistent Attention Control (VCAC) module. Given a source prompt, a target prompt and the original 3DGS  $\theta^{(0)}$  as input, the VCAC module can yield 3D-consistent and progressively edited views with a *single-step inference* to update 3DGS. Conversely, the views rendered from the updated 3DGS correct minor inconsistencies from previous view edits and serve as inputs for subsequent steps, thereby preventing error accumulation from the 2D editing process. This process alternatively update the 2D views and 3DGS in a synchronized and progressive manner, producing the final edited 3DGS  $\theta^{(T)}$ .

#### 4.1 Analysis on Optimization-based Editing

We analyze the optimization process of score distillation sampling, and generalize it to its variants. The gradient of the SDS loss function, as defined in Eq. 1, is equivalent to the gradient obtained by optimizing the rendered views to match a pseudo-ground-truth  $\hat{z}_0^{(t)}$ :

$$\begin{aligned} \nabla_{\theta} \mathcal{L}_{\text{SDS}}(\theta) &:= \mathbb{E}_{t, \epsilon, c} \left[ \omega(t) (\epsilon_{\phi}(z_t, t, y) - \epsilon) \frac{\partial g(\theta, c)}{\partial \theta} \right] \\ &= \mathbb{E}_{t, \epsilon, c} \left[ \omega(t) \frac{\sqrt{\alpha_t}}{\sqrt{1 - \alpha_t}} (z_{\pi} - \hat{z}_0^{(t)}) \frac{\partial g(\theta, c)}{\partial \theta} \right], \end{aligned} \quad (4)$$

where  $z_{\pi}$  is the rendered image's latent.

Prior works have highlighted the drawbacks of employing a uniform timestep schedule in the optimization process of SDS [8, 36, 15]. The optimization process of SDS presents a dilemma: a large noise scale is necessary in the early stages to tackle the out-of-domain issue of the rendered images. However, this large noise scale also corrupts the information of the original images, making the optimization process unstable. Therefore, it is reasonable to adopt an annealing timestep schedule so that coarse-grained structures are generated at the early stage with a large noise level, while intricate details are refined at a later stage with a lower noise level.

To further unveil the connections between SDS optimization and DDCM sampling, we make a reasonable assumption that the timestep  $t$  should follow an annealing schedule, as suggested by extensive prior research. We can write the pseudo-ground-truth as a function of the rendered image's



Figure 2: The editing trajectory exhibits a smooth and incremental transition from the original image to the final edited image.

latent  $z_\pi$ , timestep  $t$ , condition  $y$  and added noise  $\epsilon$ :

$$\begin{aligned}
 \hat{z}_0^{(t)} &:= \mathbf{f}_\phi(z_\pi, \epsilon, t, y) = \frac{(z_t - \sqrt{1 - \alpha_t} \epsilon_\phi(z_t, t, y))}{\sqrt{\alpha_t}} \\
 &= \frac{(\sqrt{\alpha_t} z_\pi + \sqrt{1 - \alpha_t} \epsilon - \sqrt{1 - \alpha_t} \epsilon_\phi(z_t, t, y))}{\sqrt{\alpha_t}} \\
 &= z_\pi + \frac{\sqrt{1 - \alpha_t}}{\sqrt{\alpha_t}} (\epsilon - \epsilon_\phi(\sqrt{\alpha_t} z_\pi + \sqrt{1 - \alpha_t} \epsilon, t, y)) .
 \end{aligned} \tag{5}$$

Note that Eq. 3 in DDCM describes the dynamics of  $z_t$ . We reparameterize it to model the dynamics of  $\hat{z}_0^{(t)}$  instead, formulated as:

$$\begin{aligned}
 \hat{z}_0^{(t)} &= \frac{z_t - \sqrt{1 - \alpha_t} \epsilon_\phi}{\sqrt{\alpha_t}} = \frac{\sqrt{\alpha_t} \hat{z}_0^{(t+1)} + \sqrt{1 - \alpha_t} \epsilon_{t+1} - \sqrt{1 - \alpha_t} \epsilon_\phi}{\sqrt{\alpha_t}} \\
 &= \hat{z}_0^{(t+1)} + \frac{\sqrt{1 - \alpha_t}}{\sqrt{\alpha_t}} (\epsilon_{t+1} - \epsilon_\phi) .
 \end{aligned} \tag{6}$$

We observe that the dynamics described by Eq. 6 closely resembles the optimization of SDS Eq. 5. With the assumption that SDS following an annealing timestep schedule, the SDS optimization is equivalent to an *iterative reconstruction* procedure: **1)** sample next-step pseudo-ground-truth using noisy latents produced from previous rendered images with DDCM; **2)** optimize a reconstruction loss to match the view with pseudo-ground-truth. This finding allows us to consider the design of 3D editing methods from a more general *iterative reconstruction* perspective. We expand this formulation to include variants of SDS, summarizing their pseudo-ground-truth parameterizations in Table ?? of the Appendix.

## 4.2 Trajectory-Anchored Scheme for Progressive 3D Gaussian Editing

Our previous analysis in Sec. 4.1 bridges the gap between *optimization-based* and *reconstruction-based* 3D Gaussian editing methods, demonstrating that optimization-based approaches are special cases of reconstruction-based methods. Without loss of generality, we consider the design of 3D editing methods from a broader *reconstruction-based* perspective. The key questions for designing improved 3D Gaussian editing methods become: (1) *which appropriate reconstruction pseudo-ground truths to use*, and (2) *how to schedule the reconstruction process of 3D Gaussians in a progressive manner for 3D editing*.

With this in mind, we propose a trajectory-anchored progressive 3D Gaussian editing scheme, as shown in Figure 1. This approach more tightly couples the image editing process with the rendering process, enabling 3D rendering to actively rectify the inconsistencies in the progressive 2D multi-view edits. Specifically, we use images generated by a modified DDCM editing trajectory, similar to InfEdit [34], as suitable pseudo-ground-truths for 3D Gaussian editing. The detailed sampling process for generating pseudo-ground-truths is described in Algorithm 1 in the Appendix. These pseudo-ground-truths enable a smooth transition from the source image to the target image (as illustrated in Figure 2), making them ideal for the progressive 2D editing and 3D updating scheme. Progressive edits on 2D views can be promptly applied to 3D Gaussians. Conversely, minor view inconsistencies arising from 2D editing can be promptly rectified through 3D constrained rendering. In line with GaussianEditor [5], we adopt a combination of reconstruction  $\mathcal{L}_1$  loss, perceptual loss  $\mathcal{L}_{\text{LPIPS}}$ , and

anchor loss  $\mathcal{L}_{\text{anchor}}$  as our loss function  $\mathcal{L}$ :

$$\mathcal{L} = \mathcal{L}_1 + \lambda_{\text{LPIPS}} \cdot \mathcal{L}_{\text{LPIPS}} + \lambda_{\text{anchor}} \cdot \mathcal{L}_{\text{anchor}} , \quad (7)$$

where  $\lambda_{\text{LPIPS}}$  and  $\lambda_{\text{anchor}}$  respectively denote the weight coefficient of perceptual loss and anchor loss.

### 4.3 View-Consistent Attention Control

Ensuring consistent edits across multiple views is crucial for effective optimization of 3D Gaussians, as inconsistent edits among different views may fail to consolidate in 3D scenes [10]. To address this, we proposed a dual-branch editing scheme that utilizes structural information from the original views as 3D view prior, imposing structural constraints on the spatial layouts of the target views. Furthermore, we employed KV propagation and KV reference mechanisms to enhance semantic consistencies across views.

We utilize a source branch and a target branch to achieve 3D consistent editing. The source branch takes in unedited original views, acting as a reference for the target branch, providing structural and semantic guidance for generating edited views. Previous studies have noted that the structural layout of an image is formed in the early stages of diffusion and is closely linked to self-attention queries. To ensure that the edited views produced by the target branch maintain structural multi-view consistency, we opt to inject self-attention queries from the source branch into the target branch during the early stages of diffusion (mid-bottom part of Figure 1). Specifically, denote the attention calculation as:

$$\text{Attn}(\mathbf{Q}, \mathbf{K}, \mathbf{V}) = \text{softmax} \left( \frac{\mathbf{Q}\mathbf{K}^\top}{\sqrt{d}} \right) \mathbf{V} . \quad (8)$$

The query injection is performed as:

$$\text{QInj}(\mathbf{Q}_{\text{src}}, \mathbf{Q}_{\text{tgt}}, \mathbf{K}_{\text{tgt}}, \mathbf{V}_{\text{tgt}}, t) = \begin{cases} \text{Attn}(\mathbf{Q}_{\text{src}}, \mathbf{K}_{\text{tgt}}, \mathbf{V}_{\text{tgt}}) & t \leq t_q \\ \text{Attn}(\mathbf{Q}_{\text{tgt}}, \mathbf{K}_{\text{tgt}}, \mathbf{V}_{\text{tgt}}) & t > t_q \end{cases} , \quad (9)$$

where  $t_q$  is the threshold that determines the number of steps for which the injection applies.

Maintaining structural multi-view consistency alone is insufficient; semantic multi-view consistency is also crucial. To achieve this, we implemented KV propagation and KV reference mechanisms (bottom-left of Figure 1). Given a sequence of  $N$  views  $\{\mathbf{I}^n\}_{n=1}^N$  resulting from consecutive camera motion, we divide the sequence into equal-partitioned context segments  $\{\mathbf{C}^i\}_{i=1}^L$ . Each context  $\mathbf{C}^i$  has a length of  $N/L$  frames and contains a keyframe  $\mathbf{I}_1^i$ . Views within the same context exhibit minimal movement or view shift, their semantics are relatively consistent. For views within the same context, we utilized an efficient KV propagation method, where the self-attention keys and values of the keyframe  $\{\mathbf{K}_1^i, \mathbf{V}_1^i\}$  of  $i$ -th context is directly propagated to the rest of the frames in the same context. Denote the output of self-attention of  $j$ -th frame in context  $i$  as  $\mathbf{O}_j^i$ , we can formulate this attention propagation as:

$$\mathbf{O}_j^i = \text{Attn}(\mathbf{Q}_j^i, \mathbf{K}_1^i, \mathbf{V}_1^i) . \quad (10)$$

Significant view shifts can occur across different contexts, leading to noticeable semantic differences. Applying KV propagation on keyframes across different contexts would accumulate significant distortion. To mitigate this, we employ KV reference for keyframes across contexts. This involves inflating the self-attention keys and values across keyframes of different contexts and processing them jointly. The self-attention keys and values from other keyframes serve as a mutual reference for the semantic information of the edited entity. For self-attention keys  $\{\mathbf{K}^i\}_{i=1}^l$  and values  $\{\mathbf{V}^i\}_{i=1}^l$  from  $l$  different keyframes, we concatenate them respectively to form cross-context KV pairs. The operation is formulated as:

$$\mathbf{O}_1^i = \text{Attn}(\mathbf{Q}_1^i, [\mathbf{K}^1, \dots, \mathbf{K}^l], [\mathbf{V}^1, \dots, \mathbf{V}^l]) . \quad (11)$$

To maintain fidelity with the original images in the non-edited areas, we applied a cross-attention control (bottom-right of Figure 1) and local blending strategy similar to Prompt-to-Prompt [14] and InfEdit [34]. Cross-attention control is done by replacing the attention maps corresponding to non-edited tokens in the target branch with those from the source branch. We use the semantic mask  $\mathbf{M}$  obtained from semantic tracing [5] to blend noisy target latent with source latent, formulated as:

$$\mathbf{z}_t^{\text{tgt}} = \mathbf{M} \odot \mathbf{z}_t^{\text{tgt}} + (1 - \mathbf{M}) \odot \mathbf{z}_t^{\text{src}} , \quad (12)$$

where  $\odot$  is the Hadamard product. Consequently, the 3D consistent view edits consolidate onto the 3D Gaussians in a rectified and progressive manner.

Table 1: Quantitative Results. Compared to DDS and GaussianEditor, our method outperforms across evaluated metrics.

Methods	Reference	CLIP Score [2]	CLIP Directional Score [2]	User Study
DDS [13]	ICCV (2023)	0.2242	0.1336	5.59%
GaussianEditor [5]	CVPR (2024)	0.2343	0.1548	25.47%
<b>TrAME (Ours)</b>	Ours	<b>0.2550</b>	<b>0.2002</b>	<b>68.94%</b>

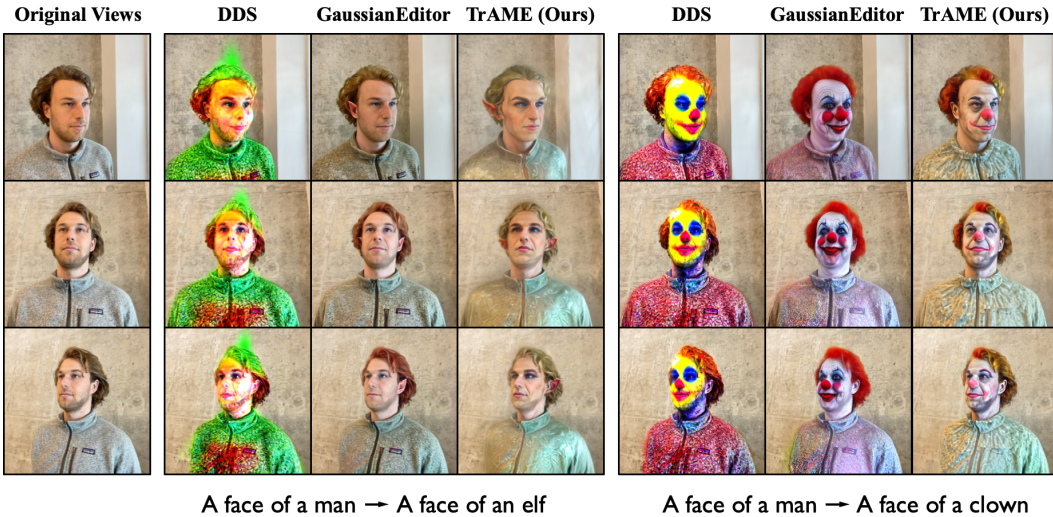


Figure 3: Qualitative comparison. A comparative analysis of experimental results for single-scene editing across State-of-the-Art methods and ours under identical conditions.

## 5 Experiments

In this section, we provide a comprehensive overview of our experimental setup, which encompasses the testing data, baseline methods and implementation details. We examine the effectiveness of our method with quantitative and qualitative results. Additionally, we conduct ablation studies on each proposed component to dissect their individual contributions to the overall performance.

### 5.1 Implementation Details

We implement our method based on a modified version of GaussianEditor [5]. Each editing typically takes about 5-15 minutes on average, depending on the complexity of the scene. For scenes involving partial editing, we adhere to the semantic tracing approach outlined in GaussianEditor. The context length of the VCAC module is set to 4. A view angle difference threshold of 25 degrees is set to determine if the displacement between two views is too large, thereby deciding whether to use the KV propagation or KV reference approach in the VCAC module. We evaluate our method on Instruct-N2N [10] and MipNeRF-360 [1] dataset. The experiments are conducted using a single Nvidia A100 80G GPU, with VRAM consumption around 30GB.

### 5.2 Baseline Methods

We compare our method with two state-of-the-art 3DGS editing methods: (1) Delta Distillation Sampling (DDS)[13], which represents the SDS optimization strategy for editing and uses an implicit score function loss derived from a diffusion model as guidance; (2) GaussianEditor [5], which represents an editing method based on Instruct-P2P [2], guiding the editing of the 3D Gaussian Splatting (3DGS) by iteratively updating the training set. Note that other 3D scene editing methods either lack publicly available code or utilize 3D representations other than 3DGS. We conduct a quantitative comparison using the CLIP Score and CLIP Directional Score [2] to evaluate the visual resemblance between the edited 3DGS and the given prompt. Additionally, we carry out a user study aimed at assessing the effectiveness of these editing methods from a human perspective.



Figure 4: Qualitative comparison. A comparative analysis of experimental results for various scenes encompassing both partial and global editing under identical conditions.

### 5.3 Quantitative Results

In our quantitative analysis, we employ the CLIP Score and CLIP Directional Score [2] to assess the alignment of the edited 3D models with the target text prompts on the rendered views of the edited 3DGS. These results indicate that our 3D editing method is effective at consolidating user edits into 3D scenes. To further validate our approach, we organized a user study involving 23 participants over 14 different cases, where users were asked to evaluate and choose the best edits based on image quality, alignment with the target prompt, and consistency across different views. The quantitative evaluation results, presented in Table 1, compare our method against baseline methods across various test scenes. Our method excels in CLIP Score, CLIP Directional Score, and user study scores, confirming its superior editing outcomes.

### 5.4 Qualitative Results

As shown in Figure 3 and Figure 4, our qualitative analysis showcases that our method ensures multi-view consistency and fine-grained details in 3D scene editing. We display outcomes from various perspectives in different scenes, underscoring the effectiveness of our method. Based on the results, we can observe that DDS faces challenges in achieving detailed and faithful editing. GaussianEditor struggles with maintaining multi-view consistency, as seen in inconsistencies such as the hair color of the elf and the nose of the clown when viewed from different angles, and in consolidating fine-grained details onto 3D textures, such as accumulated snow on park benches and patterns on marble tables (examples shown in the second and third columns of Figure 4). This shortcoming of the compared methods becomes particularly apparent when trying to capture the intricate patterns and fine details inherent to such materials, highlighting a critical area where our approach excels in producing view-consistent and detailed 3D scene edits.

### 5.5 Ablation Studies

**Study on VCAC.** The results presented in Figure 5 demonstrate that the VCAC module effectively enhances cross-view structural and semantic consistency. The views modified by our VCAC module align more accurately with the original views in terms of structural elements like poses and facing directions, and they also demonstrate better semantic coherence, exhibiting similar appearances. In particular, the outputs generated by our VCAC module maintain a uniform appearance across various



Figure 5: Ablation study on the VCAC module for 2D view editing. The results display edited views with (w. VCAC) and without the VCAC module (w/o VCAC).



Figure 6: Ablation study on TAS for 3DGS editing. Comparative results are shown with (w. TAS) and without the adoption of the TAS (w/o TAS).

views, with the facing direction of Spiderman in the figures aligning cohesively with the pose of the man in the original views.

**Study on TAS.** The ablated results obtained without TAS were derived by applying 3D editing solely based on the final obtained edited views, without feedback from the 3D Gaussians. The results depicted in Figure 6 show that TAS produces more naturalistic and consistent appearances, while the ablated results exhibit undesirable blurry artifacts and inconsistencies across views. Specifically, the hair color around the clown’s forehead in the ablated results varies across views, and the lips of the clown show ghosting shadows.

## 6 Conclusion and Future Work

Our research introduces TrAME, a progressive 3DGS editing framework that effectively improves multi-view consistency via Trajectory Anchored Scheme (TAS) and View-Consistent Attention Control (VCAC) module. Our work bridges the gap between optimization-based and reconstruction-based editing methods, offering a unified perspective for selecting better design choices in 3D scene editing methods. Our limitations reside in complex view-consistent edits with large object deformations, which will be the focus of our future work.

## References

- [1] Jonathan T Barron, Ben Mildenhall, Dor Verbin, Pratul P Srinivasan, and Peter Hedman. Mip-nerf 360: Unbounded anti-aliased neural radiance fields. In *IEEE Conf. Comput. Vis. Pattern Recog.*, pages 5470–5479, 2022.
- [2] Tim Brooks, Aleksander Holynski, and Alexei A. Efros. Instructpix2pix: Learning to Follow Image Editing Instructions. In *IEEE Conf. Comput. Vis. Pattern Recog.*, pages 18392–18402. IEEE, 2023.
- [3] Guikun Chen and Wenguan Wang. A survey on 3d gaussian splatting. *arXiv preprint arXiv:2401.03890*, 2024.
- [4] Hansheng Chen, Ruoxi Shi, Yulin Liu, Bokui Shen, Jiayuan Gu, Gordon Wetzstein, Hao Su, and Leonidas J. Guibas. Generic 3d Diffusion Adapter Using Controlled Multi-View Editing. *ArXiv*, abs/2403.12032, 2024.
- [5] Yiwen Chen, Zilong Chen, Chi Zhang, Feng Wang, Xiaofeng Yang, Yikai Wang, Zhongang Cai, Lei Yang, Huaping Liu, and Guosheng Lin. Gaussianeditor: Swift and controllable 3d editing with gaussian splatting. In *IEEE Conf. Comput. Vis. Pattern Recog.*, 2024.
- [6] Frank Dellaert and Lin Yen-Chen. Neural volume rendering: Nerf and beyond. *arXiv preprint arXiv:2101.05204*, 2020.
- [7] Kyle Gao, Yina Gao, Hongjie He, Dening Lu, Linlin Xu, and Jonathan Li. Nerf: Neural radiance field in 3d vision, a comprehensive review. *arXiv preprint arXiv:2210.00379*, 2022.
- [8] Alexandros Graikos, Nikolay Malkin, Nebojsa Jojic, and Dimitris Samaras. Diffusion Models as Plug-and-Play Priors. In *Adv. Neural Inform. Process. Syst.*, 2022.
- [9] Ayaan Haque, Matthew Tancik, Alexei A. Efros, Aleksander Holynski, and Angjoo Kanazawa. Instruct-nerf2nerf: Editing 3d scenes with instructions. In *Int. Conf. Comput. Vis.*, pages 19740–19750, October 2023.
- [10] Ayaan Haque, Matthew Tancik, Alexei A. Efros, Aleksander Holynski, and Angjoo Kanazawa. Instruct-NeRF2NeRF: Editing 3d Scenes with Instructions. In *Int. Conf. Comput. Vis.*, pages 19683–19693, 2023.
- [11] Runze He, Shaofei Huang, Xuecheng Nie, Tianrui Hui, Luoqi Liu, Jiao Dai, Jizhong Han, Guanbin Li, and Si Liu. Customize your nerf: Adaptive source driven 3d scene editing via local-global iterative training. *arXiv preprint arXiv:2312.01663*, 2023.
- [12] Yisheng He, Weihao Yuan, Siyu Zhu, Zilong Dong, Liefeng Bo, and Qixing Huang. Freditor: High-fidelity and transferable nerf editing by frequency decomposition. *arXiv preprint arXiv:2404.02514*, 2024.
- [13] Amir Hertz, Kfir Aberman, and Daniel Cohen-Or. Delta Denoising Score. In *Int. Conf. Comput. Vis.*, pages 2328–2337. IEEE, 2023.
- [14] Amir Hertz, Ron Mokady, J. Tenenbaum, Kfir Aberman, Y. Pritch, and D. Cohen-Or. Prompt-to-Prompt Image Editing with Cross-Attention Control. 2022.
- [15] Yukun Huang, Jianan Wang, Yukai Shi, Xianbiao Qi, Zheng-Jun Zha, and Lei Zhang. Dream-time: An Improved Optimization Strategy for Text-to-3d Content Creation. In *Int. Conf. Learn. Represent.*, 2024.
- [16] Hiromichi Kamata, Yuiko Sakuma, Akio Hayakawa, Masato Ishii, and Takuya Narihira. Instruct 3d-to-3d: Text instruction guided 3d-to-3d conversion. *arXiv preprint arXiv:2303.15780*, 2023.
- [17] Bernhard Kerbl, Georgios Kopanas, Thomas Leimkühler, and George Drettakis. 3d gaussian splatting for real-time radiance field rendering. *ACM Trans. Graph.*, 42(4):1–14, 2023.
- [18] Umar Khalid, Hasan Iqbal, Nazmul Karim, Jing Hua, and Chen Chen. Latenteditor: Text driven local editing of 3d scenes. *arXiv preprint arXiv:2312.09313*, 2023.

- [19] Juil Koo, Chanho Park, and Minhyuk Sung. Posterior distillation sampling. *arXiv preprint arXiv:2311.13831*, 2023.
- [20] Yuhan Li, Yishun Dou, Yue Shi, Yu Lei, Xuanhong Chen, Yi Zhang, Peng Zhou, and Bingbing Ni. Focaldreamer: Text-driven 3d editing via focal-fusion assembly. In *AAAI Conf. on Artificial Intell.*, 2024.
- [21] Ben Mildenhall, Pratul P Srinivasan, Matthew Tancik, Jonathan T Barron, Ravi Ramamoorthi, and Ren Ng. Nerf: Representing scenes as neural radiance fields for view synthesis. *Communications of the ACM*, 65(1):99–106, 2021.
- [22] Ashkan Mirzaei, Riccardo De Lutio, Seung Wook Kim, David Acuna, Jonathan Kelly, Sanja Fidler, Igor Gilitschenski, and Zan Gojcic. Reffusion: Reference adapted diffusion models for 3d scene inpainting. *arXiv preprint arXiv:2404.10765*, 2024.
- [23] Thomas Müller, Alex Evans, Christoph Schied, and Alexander Keller. Instant neural graphics primitives with a multiresolution hash encoding. *ACM Trans. Graph.*, 41(4):1–15, 2022.
- [24] JangHo Park, Gihyun Kwon, and Jong Chul Ye. Ed-nerf: Efficient text-guided editing of 3d scene with latent space nerf. In *Int. Conf. Learn. Represent.*, 2024.
- [25] Ben Poole, Ajay Jain, Jonathan T. Barron, and Ben Mildenhall. Dreamfusion: Text-to-3d using 2d Diffusion. In *Int. Conf. Learn. Represent.*, 2023.
- [26] Robin Rombach, Andreas Blattmann, Dominik Lorenz, Patrick Esser, and Björn Ommer. High-resolution image synthesis with latent diffusion models. In *IEEE Conf. Comput. Vis. Pattern Recog.*, pages 10684–10695, 2022.
- [27] Etai Sella, Gal Fiebelman, Peter Hedman, and Hadar Averbuch-Elor. Vox-e: Text-guided voxel editing of 3d objects. In *Int. Conf. Comput. Vis.*, pages 430–440, 2023.
- [28] Jiaming Song, Chenlin Meng, and Stefano Ermon. Denoising Diffusion Implicit Models. In *Int. Conf. Learn. Represent.*, 2021.
- [29] Liangchen Song, Liangliang Cao, Jiatao Gu, Yifan Jiang, Junsong Yuan, and Hao Tang. Efficient-nerf2nerf: Streamlining text-driven 3d editing with multiview correspondence-enhanced diffusion models. *arXiv preprint arXiv:2312.08563*, 2023.
- [30] Haochen Wang, Xiaodan Du, Jiahao Li, Raymond A. Yeh, and Greg Shakhnarovich. Score Jacobian Chaining: Lifting Pretrained 2d Diffusion Models for 3d Generation. In *IEEE Conf. Comput. Vis. Pattern Recog.*, pages 12619–12629. IEEE, 2023.
- [31] Peng Wang, Lingjie Liu, Yuan Liu, Christian Theobalt, Taku Komura, and Wenping Wang. Neus: Learning neural implicit surfaces by volume rendering for multi-view reconstruction. In M. Ranzato, A. Beygelzimer, Y. Dauphin, P.S. Liang, and J. Wortman Vaughan, editors, *Adv. Neural Inform. Process. Syst.*, volume 34, pages 27171–27183. Curran Associates, Inc., 2021.
- [32] Jing Wu, Jia-Wang Bian, Xinghui Li, Guangrun Wang, Ian Reid, Philip Torr, and Victor Adrian Prisacariu. Gaussctrl: Multi-view consistent text-driven 3d gaussian splatting editing. *arXiv preprint arXiv:2403.08733*, 2024.
- [33] Tong Wu, Yu-Jie Yuan, Ling-Xiao Zhang, Jie Yang, Yan-Pei Cao, Ling-Qi Yan, and Lin Gao. Recent advances in 3d gaussian splatting. *arXiv preprint arXiv:2403.11134*, 2024.
- [34] Sihan Xu, Yidong Huang, Jiayi Pan, Ziqiao Ma, and Joyce Chai. Inversion-Free Image Editing with Natural Language. In *IEEE Conf. Comput. Vis. Pattern Recog.*, 2024.
- [35] Mingqiao Ye, Martin Danelljan, Fisher Yu, and Lei Ke. Gaussian grouping: Segment and edit anything in 3d scenes. *arXiv preprint arXiv:2312.00732*, 2023.
- [36] Xuanyu Yi, Zike Wu, Qingshan Xu, Pan Zhou, Joo-Hwee Lim, and Hanwang Zhang. Diffusion Time-step Curriculum for One Image to 3d Generation. 2024.
- [37] Kai Zhang, Gernot Riegler, Noah Snaveley, and Vladlen Koltun. Nerf++: Analyzing and improving neural radiance fields. *arXiv preprint arXiv:2010.07492*, 2020.

- [38] Lvmin Zhang, Anyi Rao, and Maneesh Agrawala. Adding conditional control to text-to-image diffusion models. In *Int. Conf. Comput. Vis.*, volume abs/2302.05543, pages 3836–3847, 2023.
- [39] Xingcheng Zhou, Ying He, F Richard Yu, Jianqiang Li, and You Li. Repaint-nerf: Nerf editing via semantic masks and diffusion models. In *Int. Joint Conf. on Artificial Intell.*, pages 1813–1821, 2023.
- [40] Junzhe Zhu, Peiye Zhuang, and Sanmi Koyejo. HIFA: High-fidelity text-to-3d generation with advanced diffusion guidance. In *Int. Conf. Learn. Represent.*, 2024.
- [41] Jingyu Zhuang, Chen Wang, Liang Lin, Lingjie Liu, and Guanbin Li. Dreameditor: Text-driven 3d scene editing with neural fields. In *SIGGRAPH Asia 2023 Conference Papers*, pages 1–10, 2023.
- [42] Qi Zuo, Xiaodong Gu, Lingteng Qiu, Yuan Dong, Zhengyi Zhao, Weihao Yuan, Rui Peng, Siyu Zhu, Zilong Dong, Liefeng Bo, and Qixing Huang. Videomv: Consistent Multi-View Generation Based on Large Video Generative Model. *arXiv*, abs/2403.12010, 2024.